Small scales and anisotropy in low Rm magnetohydrodynamic turbulence

Cite as: Physics of Fluids **15**, 3170 (2003); https://doi.org/10.1063/1.1601222
Submitted: 14 February 2003 • Accepted: 24 June 2003 • Published Online: 05 September 2003

A. Pothérat and T. Alboussière

Small scales and anisotropy in low *Rm* magnetohydrodynamic turbulence

A. Pothérat and T. Alboussière
Department of Engineering, Cambridge University, Trumpington Street, Cambridge CB2 1PZ, United Kingdom

(Received 14 February 2003; accepted 24 June 2003; published 5 September 2003)

In this paper, we derive estimates for size of the small scales and the attractor dimension in low *Rm* magnetohydrodynamic turbulence by deriving a rigorous upper bound of the dimension of the attractor representing this flow. To this end, we find an upper bound for the maximum growth rate of any *n*-dimensional volume of the phase space by the evolution operator associated to the Navier–Stokes equations. As explained in Constantin *et al.* [J. Fluid Mech. **150**, 427 (1985)], the value of *n* for which this maximum is zero is an upper bound for the attractor dimension. In order to use this property in the more precise case of a three-dimensional periodical domain, we are led to calculate the distribution of *n* modes which minimizes the total (viscous and Joule) dissipation. This set of modes turns out to exhibit most of the well known properties of magnetohydrodynamic turbulence, previously obtained by heuristic considerations such as the existence of the Joule cone under strong magnetic field. The sought estimates for the small scales and attractor dimension are then obtained under no physical assumption as functions of the Hartmann and the Reynolds numbers and match the Hartmann number dependency of heuristic results. A necessary condition for the flow to be tridimensional and anisotropic (as opposed to purely two-dimensional) is also built. [DOI: 10.1063/1.1601222]

I. INTRODUCTION

Magnetohydrodynamic (MHD) turbulence at low magnetic Reynolds number *Rm* (i.e., for which the magnetic field is not disturbed by the flow) is of great interest for laboratory experiments as well as for industrial applications including metallurgy and the study of liquid metal blankets used in nuclear fusion reactors. It essentially differs from classical hydrodynamic turbulence by the additional Joule dissipation arising from the electric currents present in the flow.[1,2] This anisotropic dissipation competes with the usual viscous dissipation and when it is dominant, the flow exhibits very characteristic features: first, the turbulent modes are confined outside the so-called Joule cone in the Fourier space (of axis the direction of the applied magnetic field, and the angle of which is governed by the ratio of the Lorentz to the inertial forces). Also the additional dissipation leads to a faster energy decay proportional to $t^{-1/2}$ for freely decaying turbulence[3] when it is much greater than viscous dissipation. Homogeneous 3D MHD turbulence also exhibits a k^{-3} power density spectrum, different from the usual $k^{-5/3}$ law. This spectrum has been observed experimentally and heuristic considerations suggest it results from a local balance between inertia and Lorentz forces.[4] One of the most striking features of low-*Rm* MHD turbulence is its anisotropy due to the fact that vortices stretched along the magnetic field lines escape ohmic dissipation,[5,6] and which results in the existence of the Joule cone in Fourier space where the modes are strongly dissipated. The flow may then become two-dimensional when the modes with a nonzero wave number component in the magnetic field direction are all killed by Joule dissipation.

To summarize, three points characterize well low *Rm* MHD turbulence (this does not extend to moderate and high *Rm* MHD turbulence): its faster decay, its anisotropy, and its power density spectrum. Although all those quantities are known through experiments and relate well to heuristic considerations, none of them is clearly linked to the mathematical properties of the Navier–Stokes equations. This point is important for two reasons: first, results derived from mathematical properties of the equations are very robust and therefore give indisputable support to heuristic arguments, should they match. Second, they provide some deep insights into the behavior of the solutions, which is necessary when one wants to undertake calculations on turbulent flows. We aim at doing a step towards filling this gap by studying anisotropy and small scales in a fully established turbulent flow, by means of the theory of dynamical systems. This latter tool is indeed very suitable to understand turbulence as some of its objects are in direct relation with characteristic properties of turbulence such as the size of the smallest scales which is expressed by the idea that the solutions of Navier–Stokes are described by a finite (but possibly large) number of determining modes. This number is also of the same order of magnitude as the dimension of the attractor of the system for which estimates can be found. Some important questions then arise: (1) how many modes are required to describe the flow? (2) which modes? and (3) what information is lost if one attempts a calculation using a smaller number of modes? The purpose of this paper is to suggest some ideas for (1) and (2) in the case of MHD turbulence. A way to answer (1) is to find an upper bound for the dimension of the attractor of the dynamical system formed by the anisotropic Navier–Stokes equation (i.e., with Lorentz force) and associated boundary conditions. This work has already

been carried out without magnetic field by Ref. 7 who found a close bound for the attractor dimension of the 2D problem under the form $\mathcal{G}^{2/3}(1+\ln\mathcal{G})^{1/3}$ ($\mathcal{G}$ is the Grashof number based on a measure of the applied forcing), which fits well with the typical size of the small scales given by Ref. 8 from heuristic considerations. A similar result has been found in 3D by Ref. 9 and summarized in Ref. 10 but the final Re^3 bound found for the attractor dimension (Re is the Reynolds number) is not as sharp as the previous bound, when compared to the $\mathrm{Re}^{9/4}$ estimate by the Kolmogorov theory. However, some estimates for the inertial terms derived from this reference will be used to tackle the MHD problem. Note that a thorough study of the general MHD equations (i.e., the system formed with the Navier–Stokes equations and the induction equations, which covers situations where velocity and magnetic field are fully coupled) is presented in Ref. 11. In particular, it is shown that any invariant set for this system (hence any attractor) has a finite Hausdorf dimension. Note also that MHD turbulence where the magnetic field can fluctuate has been widely studied and even if the physical mechanisms involved are very different to those in the case we study here, a similar anisotropy is observed when a mean magnetic field is imposed (see, for instance, Ref. 12).

The layout of the paper is as follows: we first review the tools of system dynamics used thereafter (i.e., the method for calculating the attractor dimension) and show how they relate to our problem. It turns out that calculating the upper bound for the attractor dimension is related to the problem of finding the least dissipative modes. Section III is devoted to finding those modes and their properties as well as the upper bound itself: those modes are found to correspond to prominent modes of actual MHD-turbulent flows. In Sec. IV, analytical estimates are given and a comparison is drawn with the usual heuristic arguments.

II. NAVIER–STOKES EQUATIONS AND DYNAMICAL SYSTEMS

A. Method for calculating an upper bound for the attractor dimension of a dynamical system

We shall now give some guidelines about the method which we use to derive such an upper bound. A dynamical system with vector valuated unknown $\mathbf{x}$ is defined by an evolution equation of the form

$$\frac{d\mathbf{x}}{dt}=F(\mathbf{x}) \tag{1}$$

together with boundary conditions on the considered domain spanned by the variable $\mathbf{x}$ or phase space. By definition of a global attractor for the system (which is a set located in the phase space), a solution of Eq. (1) always ends up being arbitrary close to it at infinite time. Therefore, if we consider any set of n infinitesimal independent departures from a solution located in the attractor $(\delta\mathbf{x}_k)_{k=1\ldots n}$, the subset of the phase space generated by these disturbances will eventually end up within the attractor in the limit $t\to\infty$. This implies that if the initial dimension n of this subset is greater than the attractor dimension, its n-dimensional volume tends to zero at infinite time (as, for instance, a 3D cube would have to become "flat," i.e., of volume 0, in order to fit in a plane at infinite time). Therefore, the lowest value of n for which the volume of the subspace generated by any set of n disturbances annihilates at infinite time is an upper bound for the attractor dimension. This result is expressed rigorously and extended to noninteger values of n by the theorem of Constantin and Foias.[13]

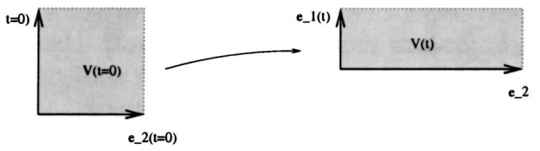

FIG. 1. Evolution of the volume associated with a base of orthogonal eigenvectors of an operator in the phase space. The dimension n is set to 2.

In order to be able to use this theorem, it suffices to find the lowest value of n which corresponds to a zero value of the maximum expansion rate among all possible n-dimensional infinitesimal disturbances. The evolution of each disturbance is expressed by linearization of Eq. (1) in the vicinity of the attractor:

$$\frac{d}{dt}\delta\mathbf{x}=\mathcal{A}\delta\mathbf{x}+O(\delta\mathbf{x}^2). \tag{2}$$

Then the expansion rate of the n-volume $V_n=\|\delta\mathbf{x}_1\times\ldots\times\delta\mathbf{x}_n\|$ is the sum of the expansion rates in all the eigendirections of $\mathcal{A}$ within the n-dimensional subspace:

$$V_n(t)=V_n(t=0)\exp(t\langle\mathrm{Tr}[\mathcal{A}\mathbf{P}_n]\rangle_t), \tag{3}$$

where $\mathbf{P}_n$ stands for the projector onto the n dimensional subspace spanned by $(\delta\mathbf{x}_k(t))_{k=1\ldots n}$, and $\langle\,\rangle_t$ stands for the longest possible time-average. One can get an idea of how this result comes up by considering the volume spanned by a base of orthogonal eigenvectors of $\mathcal{A}$ $(\mathbf{e}_k)_{k\in\{1\ldots n\}}$, in the case where $\mathcal{A}$ is self-adjoint and time-independent. If $(\lambda_k)_{k\in\{1\ldots n\}}$ is the related set of eigenvalues, then the length of the volume element along the direction $\mathbf{e}_k$ evolves as (see Fig. 1)

$$\mathbf{e}_k(t)=\mathbf{e}_k(t=0)\exp(\lambda_k t). \tag{4}$$

As the $(\mathbf{e}_k)$ are orthogonal, the volume is simply the product of the lengths in all directions, so that it evolves as

$$V_n=\|\mathbf{e}_1(t=0)\|\|\mathbf{e}_2(t=0)\|\ldots\|\mathbf{e}_n(t=0)\|\exp\left(\sum_{k=1\ldots n}\lambda_k t\right)$$

$$=V_n(t=0)\exp(\mathrm{Tr}\,\mathcal{A}t). \tag{5}$$

Finding the maximum expansion rate over every possible n-dimensional subspace then comes down to finding the maximum of the trace of the linearized evolution operator over all possible sets of n of its eigenmodes. Let us now apply these ideas to the problem of MHD turbulence.

B. The Navier–Stokes equations as a dynamical system

Let us consider an incompressible electrically conducting fluid in a finite domain, subject to a permanent, uniform magnetic field $\mathbf{B}$ aligned with the z-axis. If σ is the electrical

conductivity, ρ is the density, ν is the kinematic viscosity, the motion equations for velocity $\mathbf{u}$, pressure p electric current density $\mathbf{j}$ can be written

$$(\partial_t+\mathbf{u}\cdot\nabla)\mathbf{u}+\frac{1}{\rho}\nabla p=\nu\left(\nabla^2\mathbf{u}+\frac{1}{\rho\nu}\mathbf{j}\times\mathbf{B}\right)+\mathbf{f}, \tag{6}$$

$$\nabla\cdot\mathbf{u}=0, \tag{7}$$

where $\mathbf{f}$ represents some forcing independent of the velocity field. The set of Maxwell equations as well as electric current conservation and the Ohm's law are normally required to close the system. However, we assume here that the magnetic field is not disturbed by the flow. In other words, the magnetic diffusion is supposed to take place instantaneously at the time scale of the flow (''low magnetic Reynolds number'' approximation). In this case, Ref. 14 has shown that the Lorentz force decomposes as the sum of a magnetic pressure term and a rotational term:

$$\mathbf{j}\times\mathbf{B}=\frac{\nu}{\rho}\nabla p_m+\frac{\sigma B^2}{\rho\nu}\nabla^{-2}\partial_{zz}^2\mathbf{u}. \tag{8}$$

This reveals the nature of the electromagnetic effects on the flow: the first term accounts for the electromagnetic pressure (of little effect in incompressible flows). The second term can be interpreted as a momentum diffusion along the magnetic field lines[5] which tends to homogenize x, y components of the velocity along z. This stretches vortices along the z direction. The actual turbulent flow therefore exhibits some anisotropy which results from the competition between this momentum diffusion and the tendency from inertial terms to favor return to isotropy. Note that if the electromagnetic effects are dominant, the stretched vortices can reach the boundaries of the flow, which then becomes two-dimensional.

Injecting Eq. (8) in the Navier–Stokes equation (6), the electromagnetic pressure is absorbed in the hydrodynamic pressure term so that the entire MHD problem is expressed using the velocity only. The related variation equation which governs the evolution of a three-dimensional perturbation $\delta\mathbf{u}$ of the solution $\mathbf{u}$ then takes the form

$$\partial_t\delta\mathbf{u}=-\underbrace{\mathbf{u}\cdot\nabla\delta\mathbf{u}-\delta\mathbf{u}\cdot\nabla\mathbf{u}}_{\textit{non-linear inertia}}+\nu\underbrace{\left(\nabla^2+\frac{\sigma B^2}{\rho\nu}\nabla^{-2}\partial_{zz}^2\right)}_{\textit{dissipation}}\delta\mathbf{u}, \tag{9}$$

$$\nabla\cdot\delta\mathbf{u}=0. \tag{10}$$

In the literature, the nonlinear inertial terms are often written as a bilinear operator $\mathcal{B}(\mathbf{u},\delta\mathbf{u})$, and the dissipation, as a linear operator that we call $\mathcal{D}_{\mathrm{Ha}}$ (as it will be seen to depend on the Hartmann number Ha in Sec. III). One can guess from this equation, that the evolution of small volume of the phase space generated by a set of n disturbances (as defined in Sec. II A) results from the competition between inertial terms which tend to expand the volume by vortex stretching and dissipative terms which tends to damp the disturbances, and hence reduce the volume.

The case without magnetic field has been investigated in two and three dimensions. In 2D, Ref. 15 found an upper bound for the attractor dimension which matches well the results obtained by Kolmogorov-like arguments:

$$d_{2\mathrm{D}}\leqslant c_1\mathcal{G}^{2/3}(1+\ln\mathcal{G})^{1/3}, \tag{11}$$

where $\mathcal{G}$ is the Grashof number expressing the ratio of the forcing to the viscous friction and c_1, as well as every c_i introduced throughout the rest of the paper, are constants of order 1. To this day, no rigorous estimate for the attractor dimension of the 3D problem precisely matches Kolmogorov's prediction for the number of degrees of freedom. One of the main reasons is that unlike in 2D, it has not yet been proved that the velocity gradients remain finite at finite time, which lets the door open to possible singularities. However, one can work under the assumption that the flow remains regular at finite time and define the maximum local energy dissipation rate as

$$\epsilon=\nu\langle\sup_{\mathbf{u}}\sup_{\mathbf{r}}\|\nabla\mathbf{u}(\mathbf{r},t)\|^2\rangle_t. \tag{12}$$

One can also define a Reynolds number Re using a suitable velocity scale and a typical large scale L, which can be extracted from the eigenvalue of the Laplacian of smallest module λ_1, such that $L=\lambda_1^{-1/2}$:

$$\mathrm{Re}=\frac{L\langle\sup_{\mathbf{u}}\sup_{\mathbf{r}}\|\mathbf{u}(\mathbf{x},t)\|^2\rangle_t^{1/2}}{\nu}. \tag{13}$$

Here, $\sup_{\mathbf{u}}$ stands for the upper bound over the set of solutions $\mathbf{u}$ in the phase space, whereas $\sup_{\mathbf{r}}$ stands for the upper bound over the physical domain. Note that fixing the value of the Reynolds number is the 3D equivalent to fixing the value of the Grashof number, which represents the forcing in 2D. It should be underlined at this point, that as the attractor is only defined for quasi-steady states, it is entirely determined by the balance between forcing (given by the value of the Reynolds number) and dissipation (the nature of which is fixed by the value of the Hartmann number).

Under this assumption that the velocity remains finite, an upper bound for the trace of the operator $\mathcal{B}(.,\mathbf{u})$ on any n-dimensional subspace of the phase space is presented in Ref. 10:

$$|\mathrm{Tr}(\mathcal{B}(.,\mathbf{u}))|<\tfrac{1}{2}\nu\lambda_1 n\,\mathrm{Re}^2. \tag{14}$$

Also, studying the sequence of eigenvalues of the dissipation operator (which reduces to a Laplacian in the absence of magnetic field) on a finite physical domain with appropriate boundary conditions, gives access to the trace of the dissipation operator (see, for instance, Ref. 15) and provides an upper bound for the trace of the total evolution operator, on any n-dimensional subspace of the phase space:

$$\mathrm{Tr}((\mathcal{B}(.,\mathbf{u})+\nu\nabla^2)\mathbf{P}_n)\leqslant\nu\lambda_1 n(\tfrac{1}{2}\mathrm{Re}^2-c_2 n^{2/3}). \tag{15}$$

One can be sure that when n is such that the r.h.s. of Eq. (15) is negative, all n-volumes shrink, hence $n>d_{3\mathrm{D}}$ where $d_{3\mathrm{D}}$ is the attractor's dimension (this is Constantin and Foias theorem[16]). It then comes from Eq. (15) that

$$d_{3\mathrm{D}}\leqslant c_3\,\mathrm{Re}^3. \tag{16}$$

The bound (16) is a rather loose estimate when compared to the $\mathrm{Re}^{9/4}$ number of degrees of freedom derived from Kolmogorov arguments which assumes the existence of a power-law spectrum and uses a Reynolds number defined on the mean-square velocity. This is probably due to the difficulty in getting estimates for the norms of the velocity gradients, as well as to the fact that the bound given here does not rely on the existence of a power-law spectrum, which makes it also valid for low values of Re, unlike the K41[17] theory.

Coming back to the problem of finding an upper bound for the attractor of an MHD turbulent flow under imposed magnetic field, our task now consists mainly in finding an upper bound for the trace of the operator $\mathcal{D}_{\mathrm{Ha}}$ on any n-dimensional subspace, as the estimate for the inertial terms (14) can then still be used to derive the minimum of the trace of the linearized evolution operator. The study of the dissipation operator, with the aim of finding such a minimum is the purpose of Sec. III. To this end, and in order to keep the calculations simple, we shall restrict the problem to a physical domain defined by a three-dimensional periodic box of size $2\pi L$.

III. MODES MINIMIZING THE DISSIPATION

A. Eigenvalue problem for the dissipation operator

We now look for the maximum trace of the dissipation operator, or bearing in mind that this trace is negative, we aim at finding the modes with the least dissipation. The physical domain is a 3D-periodic box of size $2\pi L$ in a uniform, vertical magnetic field. Normalizing distances by L, the dissipation operator rewrites $\mathcal{D}_{\mathrm{Ha}}=(\nu/L^2)(\nabla^2+\mathrm{Ha}^2\,\nabla^{-2}\,\partial_{zz}^2)$, where the square of the Hartmann number $\mathrm{Ha}=LB\sqrt{\sigma/\rho\nu}$ represents the ratio of Joule to viscous dissipation at the largest scale L. From now on, $\mathcal{D}_{\mathrm{Ha}}$ will denote the nondimensional form of the dissipation operator, normalized by ν/L^2. It is straightforward to see that under periodic boundary conditions, the Laplacian is invertible so that $\mathcal{D}_{\mathrm{Ha}}$ is also invertible, as well as compact and self-adjoint. $\mathcal{D}_{\mathrm{Ha}}$ therefore has a discrete spectrum. Finding the minimum value of the modulus of the trace of $\mathcal{D}_{\mathrm{Ha}}$ over any n-subspace then comes down to finding the n eigenvalues of $\mathcal{D}_{\mathrm{Ha}}$ of smallest module $(\lambda_k)_{k=1\ldots n}$. In other words, we need to find the n least dissipative modes. The rest of this subsection is devoted to this task.

The eigenvalues problem for $\mathcal{D}_{\mathrm{Ha}}$ can be written

$$(\nabla^4+\mathrm{Ha}^2\,\partial_{zz}^2)\mathbf{v}=\lambda\nabla^2\mathbf{v}, \tag{17}$$

$$\nabla\cdot\mathbf{v}=0. \tag{18}$$

Under periodic boundary conditions, $\partial/\partial x$, $\partial/\partial y$, and $\partial/\partial z$ commute with $\mathcal{D}_{\mathrm{Ha}}$ so that each component v_x, v_y, and v_z of the solution $\mathbf{v}=(v_i)_{i\in\{x,y,z\}}$ of Eq. (17) is of the form

$$v_i(\mathbf{x})=V_i\exp(\mathbf{k}\cdot\mathbf{x}+\phi_i), \tag{19}$$

with

$$\mathbf{k}=(k_x,k_y,k_z)\in\mathbb{Z}^3,$$

$$\mathbf{x}=(x,y,z)\in[0\ldots 2\pi L]^3,$$

$$\phi_i\in[-\pi,\pi].$$

Note that $\mathbf{k}\neq 0$, as $\mathcal{D}_{\mathrm{Ha}}$ is invertible. The continuity equation implies that $\mathbf{k}\cdot\mathbf{V}=0$ so that eventually, the dimension of the eigenspace associated to $\mathbf{k}$ is 2. Wave numbers k_x, k_y, k_z are related to the eigenvalue λ through the dissipation equation, obtained by injecting Eq. (19) in Eq. (17):

$$\lambda(k_x,k_y,k_z)=-(k_x^2+k_y^2+k_z^2)-\mathrm{Ha}^2\frac{k_z^2}{k_x^2+k_y^2+k_z^2}. \tag{20}$$

We shall now assume that the components of $\mathbf{k}$ are positive and that one $\mathbf{k}$ actually represents 8 (resp. 4 resp. 2) different modes if $\mathbf{k}$ has no (resp. one resp. two) zero component(s), so that the eigenspace associated to $\lambda(k_x,k_y,k_z)$ has a dimension 16 (resp. 8 resp. 4). Each eigenvalue $\lambda(k_x,k_y,k_z)$ can be interpreted as the dissipation rate associated with the mode (k_x,k_y,k_z). We see that because of Joule dissipation, the total dissipation is always higher than the viscous dissipation alone (obtained for $\mathrm{Ha}=0$). Note also that as the eigenmodes are trigonometric functions, the space spanned by (k_x,k_y,k_z) is the discrete Fourier space.

B. Distribution of the least dissipative modes in the Fourier space

The n least dissipative modes are given by the n lowest values of $-\lambda(k_x,k_y,k_z)$. In order to find them, we note that $k_z\mapsto-\lambda(k_x,k_y,k_z)$ is always increasing. This implies that the n minimal modes have to be located "below" [i.e., closer to the (k_x,k_y) plane than...] the manifold $\lambda(k_x,k_y,k_z)=\lambda_m$ where $-\lambda_m(n)$ is the maximum value of $-\lambda(k_x,k_y,k_z)$ reached on the set of n minimal modes. The fact that $\partial-\lambda/\partial k_z>0$ also implies that all $\mathbf{k}$ inside the volume defined by this curve, $k_x\geqslant 0$, $k_y\geqslant 0$ and $k_z\geqslant 0$, do belong to the set of n minimal modes. [In the case where several triplets achieve the value λ_m, the curve $f=\lambda-\lambda_m$, may in fact enclose more than n points, but this little error is of no consequence for our purpose, and is anyway addressed in the numerical method described in Sec. III C.]

This provides enough information to visualize the distribution of the n minimal modes: As shown in Fig. 2, the 2D manifolds $\lambda=\lambda_m(n)$ are represented in the plane $(k_\perp,k_z)$, where $k_\perp^2=k_x^2+k_y^2$, by a family of curves $G_{\mathrm{Ha},n}$ of equation in polar coordinates:

$$G_{\mathrm{Ha},n}: r=\sqrt{-\lambda_m-\mathrm{Ha}^2\sin^2\theta}. \tag{21}$$

Note that $\lambda_m(n)$ is the value which corresponds to the nth mode as the modes are sorted by growing dissipation rate. For Ha fixed, $-\lambda_m(n)$ is thus an increasing function of n and determines uniquely the graph $G_{\mathrm{Ha},n}$ when n varies. One can then already get a quantitative picture of the set of n minimal modes and distinguish three different kinds of sets.

(1) For $\mathrm{Ha}>1$ fixed, the least dissipative modes are located on the $k_\perp$ axis, and therefore do not depend on z and correspond to a two-dimensional flow independent of z. Indeed, the function $k_\perp\mapsto\lambda(k_\perp,k_z)$, where $k_\perp=\sqrt{k_x^2+k_y^2}$, has a unique absolute minimum for $k_\perp^2=(\mathrm{Ha}-k_z)k_z$. The less dissipative mode is then $(k_\perp,k_z)=(0,1)$, as $(0,0)$ is not permitted (because $\lambda=0$ is not an eigenvalue of $\mathcal{D}_{\mathrm{Ha}}$). The first 3D mode to appear has to be the least dissipative mode such that $k_z>0$, the variations of $\lambda(k_\perp,k_z)$ imply that it is $(\mathrm{Ha}-1,1)$. If $k_{2\mathrm{D}}$ is the maximum value of $k_\perp$ among the 2D

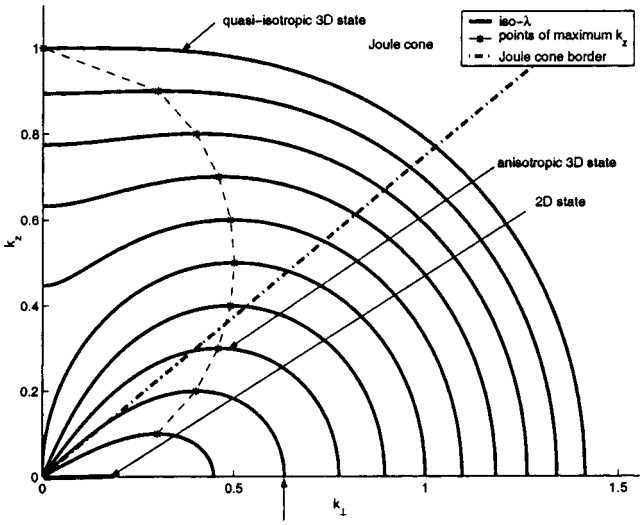

FIG. 2. Iso-λ curves in the plane $(k_\perp, k_z)$. One can see the three major types of mode distribution: the 2D state corresponds to a set of modes located on the $k_\perp$ axis, the strongly anisotropic 3D state exhibits the Joule cone-like shape (the border of the Joule cone has been plotted in the case where all the modes are inside the curve designated by the vertical arrow) and the quasi-isotropic state is reached when the modes are enclosed inside curves located the furthest away from the origin. Axis units are arbitrary. The semicircle of center (0,5,0), for which $-\lambda_m = \mathrm{Ha}^2$ is also the limit between modes described in Sec. III B (2) and modes described in Sec. III B (3).

modes, then $(k_{2D},0)$ has to be less dissipative than $(\sqrt{\mathrm{Ha}^2-1},1)$, which yields k_{2D} and the associated dissipation rate:

$$k_{2D} = \sqrt{2\,\mathrm{Ha}} - 1, \tag{22}$$

$$\lambda(\sqrt{\mathrm{Ha}-1},1) = 2\,\mathrm{Ha}. \tag{23}$$

[If $\mathrm{Ha}<1$, the second mode is 3D and is always (0,1).]

(2) The next added modes (by order of growing dissipation rate) spread inside a cardioid which is very elongated along the $k_\perp$ axis. The flow represented by such modes is therefore highly anisotropic and features vortices stretched along the z direction. Such a distribution of modes matches the well known properties of 3D turbulent flows under strong magnetic field, for which turbulent modes are located outside the so-called Joule cone of axis k_z in Fourier space.[4,5] More precisely, when $\sqrt{-\lambda_m}/\mathrm{Ha}<1$ (which can only happen for $\mathrm{Ha}>1$ for which (0,1) is not the second dissipative mode), the cardioid is located under the line $\theta=\theta_m$ where $\theta_m = \arcsin(\sqrt{-\lambda_m}/\mathrm{Ha})$, so that the volume defined by such a cardioid elongated along the $k_\perp$ axis matches well a truncation (because n is finite) of the space outside the Joule cone.

(3) Eventually, if more modes need to be added in order to reach the value of n, a value of λ_m is reached such that $\sqrt{-\lambda_m}/\mathrm{Ha}>1$, so that $0<\theta\leqslant\pi/2$. In other words, the cardioid looks more like a quarter of an ellipsoid centered around the origin, the shape of which tends toward a quarter circle as the number of modes increases and the Joule cone degenerates into the k_z axis. Such a picture describes a nearly isotropic flow, only weakly affected by electromagnetic effects. Note that unlike the 2D–3D transition, which takes place for one specific value of n at Ha fixed, the transition between 3D turbulence with a joule cone and quasi-isotropic 3D turbulence is smooth. Indeed, for $\mathrm{Ha}^2<-\lambda_m(n)<2\,\mathrm{Ha}^2$ the $G_{\mathrm{Ha},n}$ graphs look like some hybrid between a cardioid and an ellipse (see Fig. 2).

In the whole eigenvalue problem, we have assumed that n was fixed. However, for a given values of Ha and Re, n corresponds to the number of modes for which the minimal dissipation compensates the expansion of the initial n-volume in the phase space due to inertia. At fixed Ha, we can see that for low inertia (i.e., low n) the flow is two dimensional, whereas for strong inertia, the flow can be close to three-dimensional isotropic turbulence. Physically, this suggests that the flow corresponding to the estimate of the attractor dimension we are looking for results from a random production of modes by inertia [as the estimate (14) depends on the number of modes but not on their distribution in the phase space], and a selection of the least dissipative modes by the dissipative terms. Of course, this assumes that the estimate (14) for the expansion rate due to inertial effects is realistic, at least with regard to its dependency on n. At this point, it is important to recall that the minimal modes of the dissipation operator found here are not solution of the Navier–Stokes equations. However, they turn out to exhibit a physical behavior which matches qualitatively what is heuristically known from turbulent MHD flows. This suggests that expansions of solutions of the Navier–Stokes equations over the base of minimal eigenmodes of the dissipation might be suitable to calculate turbulent flows, all the more as these modes already satisfy the boundary conditions.

We shall now compute recursively the set of n least dissipative modes in the discrete space of Fourier coefficients and find the related upper bound for the attractor dimension. Note that as we actually construct an n-dimensional set of modes which achieves the maximum magnitude of the trace of $\mathcal{D}_{\mathrm{Ha}}\mathbf{P}_n$, the upper bound for the modulus of this trace actually *is* the maximum (keeping in mind that the trace of the dissipation is negative).

C. Trace of the dissipation operator and attractor dimension

We shall now calculate the trace of $\mathcal{D}_{\mathrm{Ha}}\mathbf{P}_n$ associated with the least dissipative modes as a function of n and Ha, then using Eq. (14), we express the estimate for the upper bound of the attractor dimension as a function of Ha and Re by searching the value of n which annihilates the trace of the evolution operator, as explained in Sec. II A. The trace of $\mathcal{D}_{\mathrm{Ha}}\mathbf{P}_n$ is calculated nearly exactly using a computer (the only error is due to truncation after the 17th digits of real numbers which occurs in our program) by adding up the dissipation rates along the sequence of modes sorted by increasing values of $-\lambda$. The method is described in the Appendix.

The graphs of $\mathrm{Tr}(\mathcal{D}_{\mathrm{Ha}}\mathbf{P}_n)$ and the estimate for the attractor dimension $d_M(\mathrm{Re},\mathrm{Ha})$ are reported, respectively, in Figs. 3 and 4. For now, let us put the emphasis on the curves in Fig. 4 which show the variations of the attractor dimension estimate with regard to the variable Ha, for different fixed values of the Reynolds number. Apart for very low values of the Reynolds number (of the order of unity, which does not

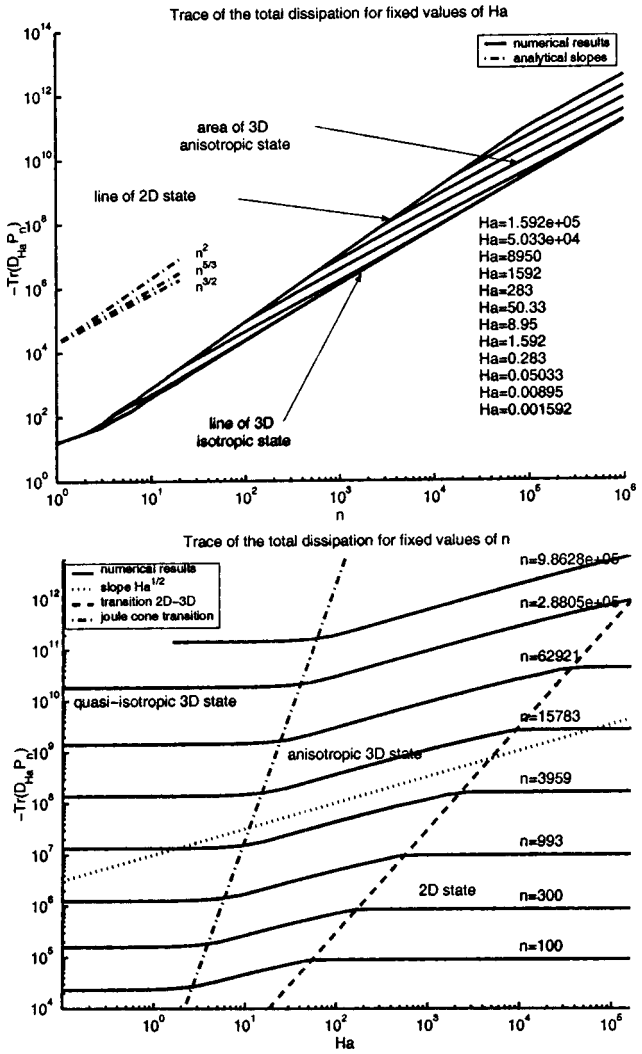

FIG. 3. Trace of the dissipation operator as a function of n for fixed Ha (top). Each iso-n curve exhibits successively n^2 (2D modes), $n^{3/2}$ (3D anisotropic set of modes) and $n^{5/3}$ slopes (quasi-isotropic set of modes). The higher the value of Ha, the later the transitions occur. The curves corresponding to the five lowest values of Ha are not distinguishable. Trace of the dissipation operator as a function of Ha for fixed n (bottom). The three different kinds of sets of modes appear (quasi-isotropic, for low Ha, 2D for high Ha).

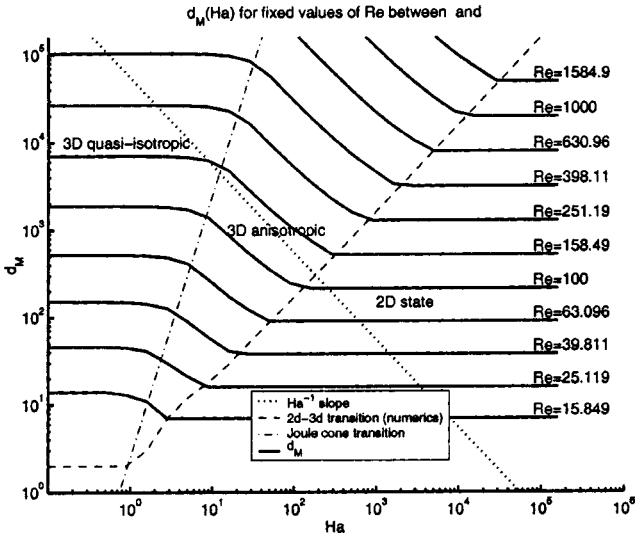

FIG. 4. Attractor dimension as a function of Ha for fixed Re.

relate to the usual picture of turbulent flows), each curve clearly exhibits three distinct regions corresponding to three different ranges of Hartmann numbers. Let us follow a given curve from Ha=0 to high values of Ha. Physically, this would correspond to looking at a turbulent flow and increasing the applied magnetic field in a quasi-static way.

(1) We first encounter a region where the attractor dimension is nearly constant when the Hartmann number increases. This region describes a flow under weak magnetic field, for which the dissipation is essentially due to viscosity, and therefore does not depend on the magnetic field. The flow is in a state of 3D quasi-isotropic turbulence and the modes are spread within a nearly circular region (of radius $k_{\perp_m} \sim k_{z_m}$) of the $(k_\perp, k_z)$ plane.

(2) For values of Ha above one, the attractor dimension decreases approximately as Ha^{-1}. Indeed, for Ha$\sim$1 viscous and Joule dissipation are of the same order of magnitude so that the overall dissipation is stronger than in the hydrodynamic case. Therefore as Re is fixed, fewer modes are needed to reach a dissipation which balances the expansion rate $n\,\mathrm{Re}$ due to inertia. Equivalently, turbulence becomes more and more anisotropic as vortices are stretched in the direction of the magnetic field, so if one interprets d_M as the number of vortices in the domain, as in Ref. 10, fewer of these long vortices are needed to fill the $2\pi L \times 2\pi L \times 2\pi L$ box, so that the number of degrees of freedom decreases. This second case corresponds to a set of modes defined by the elongated cardioid of Sec. III B.

Eventually, for even higher values of the magnetic field, one reaches a region where again, the estimate found for the attractor dimension does not depend on Ha. One can see from Fig. 4 that this happens when the flow undergoes a transition between 3D and 2D state, or in other words, when even the smallest vortex reaches the size of the box in the z direction ($k_{z_m} < 1$). The flow then becomes two-dimensional and looks like ''rows'' of columnar vortices (modes are on the $k_\perp$ axis according to the description of Sec. III B). As there is no more velocity variation along the magnetic field lines, no current loops are present in the flow so that the Lorentz force falls to 0 [looking at Eq. (8), $\partial^2_{zz}\mathbf{u}=0$ implies $\nabla\times(\mathbf{j}\times\mathbf{B})=0$]. The attractor dimension does not depend on Ha anymore but should match estimates found for two-dimensional turbulence. It does not turn out to be the case but we shall leave this point for more thorough discussion in Sec. IV.

Up to now, we have found a set of modes which corresponds to the actual minimum dissipation and which, under the assumption of finite dissipation (12), returns an upper bound for the attractor dimension of turbulent MHD flows, without any restrictions on the values of Ha and Re. What is more striking is that although these modes are not solution of the Navier–Stokes equations themselves, their distribution in the Fourier space seems to match physical observations for such turbulent flows. To find out to what extent this is the case, we shall now derive some analytical approximations of

the ''exact'' results found in this section and compare them to broadly accepted results derived from heuristic arguments.

IV. ASYMPTOTIC RESULTS AND COMPARISON WITH HEURISTICS

A. Integral formulation of the eigenvalue problem

We go back to the point where the set of n less dissipative modes is calculated, at the end of Sec. III B, and we aim at finding some analytical approximations for the results obtained numerically in Sec. III C, should it be at the price of working only in asymptotic regimes of the flow parameters. At this stage, the problem of finding the set of n eigenmodes which minimize the dissipation can be mathematically formulated as follows: for given n and Ha, we look for the set of n points $(\mathbf{k}_i)_{i=1\ldots n}$ in $\mathbb{N}^3-(0,0,0)$ which achieves the minimum of the functional:

$$\mathrm{Tr}(\mathcal{D}_{\mathrm{Ha}}\mathbf{P}_{8n})=2\sum_{i\in\{1\ldots n\}}-\lambda(\mathbf{k}_i). \tag{24}$$

The study of this set of modes in Sec. III has shown that the $(\mathbf{k}_i)_{i=1\ldots n}$ are located inside the volume V_{λ_m} located ''under'' the manifold of equation $\lambda(k_x,k_y,k_z)=\lambda_m$, which defines it uniquely (see note at the beginning of Sec. III B). The problem then comes down to expressing λ_m as a function of n and Ha. To this end, we notice that the dimension of the attractor associated with a turbulent flow is an enormous number, for which the sums [such as the one in Eq. (24)] can be safely replaced by integrals over the continuous Fourier space. Under this approximation, the fact the modes are on a discrete set implies that each of them fills a unit-volume in the Fourier space, so that the volume contained under the manifold $\lambda(x,y,z)=\lambda_m$ should be $n/8$:

$$16\int_{V_{\lambda_m}}dk_x\,dk_y\,dk_z=n. \tag{25}$$

The trace of $\mathcal{D}_{\mathrm{Ha}}\mathbf{P}_n$ similarly expresses as

$$\mathrm{Tr}(\mathcal{D}_{\mathrm{Ha}}\mathbf{P}_n)=16\int_{V_{\lambda_m}}\lambda(k_x,k_y,k_z)dk_x\,dk_y\,dk_z. \tag{26}$$

Equations (25) and (26) allow to derive both λ_m and $\mathrm{Tr}(\mathcal{D}_{\mathrm{Ha}}\mathbf{P}_n)$ as functions of n and Ha only. This can be done analytically all the way through for each of the types of minimal set of n modes found in Sec. III A. The next two sections are devoted to this task, as well as to comparing the obtained results with heuristic considerations on MHD turbulence.

B. Anisotropic turbulence under strong magnetic field

1. Analytical estimates

Let us first tackle the case where the modes are located within an elongated cardioid, i.e., $\mathrm{Ha}<-\lambda_m<\mathrm{Ha}^2$, which corresponds to a 3D anisotropic flow with dominant electromagnetic effects (see Sec. III C). After integration in cylindrical coordinates for $0<\theta<\theta_m$, Eqs. (25) and (26), respectively, take the form:

$$\frac{n}{\mathrm{Ha}^3}=\frac{\pi^2}{2}\sin^4\theta_m, \tag{27}$$

$$\frac{\mathrm{Tr}(\mathcal{D}_{\mathrm{Ha}}\mathbf{P}_n)}{\mathrm{Ha}^5}=-\frac{\pi^2}{3}\sin^6\theta_m. \tag{28}$$

Let us recall that θ_m is defined by $\sin\theta_m=\sqrt{-\lambda_m}/\mathrm{Ha}$, hence Eq. (28) allows us to express λ_m as a function of n:

$$\lambda_m=\frac{\sqrt{2}}{\pi}\mathrm{Ha}^{1/2}n^{1/2}, \tag{29}$$

and Eq. (28) allows then to express the trace of the dissipation in terms of n:

$$\mathrm{Tr}(\mathcal{D}_{\mathrm{Ha}}\mathbf{P}_n)=\frac{2\sqrt{2}}{3\pi}n^{3/2}\mathrm{Ha}^{1/2}, \tag{30}$$

$$\sin\theta_m=\sqrt{\frac{2}{\pi}}n^{1/4}\mathrm{Ha}^{-3/4}=\sqrt{\frac{-\lambda_m}{\mathrm{Ha}^2}}. \tag{31}$$

The value of n for which the trace of the total evolution operator is zero [i.e., $\mathrm{Tr}((\mathcal{D}_{\mathrm{Ha}}+\mathcal{B}(.,\mathbf{u})\mathbf{P}_n))=0$] is an upper bound for the attractor dimension, so using Eq. (14):

$$d_M\leqslant\frac{9\pi^2}{32}\frac{\mathrm{Re}^4}{\mathrm{Ha}}. \tag{32}$$

The geometrical shape of the cardioid which defines the set of n minimal modes yield the maximum values reached by $k_\perp$ and k_z, respectively:

$$k_{\perp_m}=\sqrt{-\lambda_m}=\frac{2^{1/4}}{\pi^{1/2}}n^{1/4}\mathrm{Ha}^{1/4}, \tag{33}$$

$$k_{z_m}=-\frac{\lambda_m}{2\,\mathrm{Ha}}=\frac{1}{\pi\sqrt{2}}n^{1/2}\mathrm{Ha}^{-1/2}. \tag{34}$$

The bounds for the size of the small scales are obtained by replacing n by d_M, Eqs. (33) and (34), respectively:

$$k_{\perp_m}\leqslant\frac{\sqrt{3}}{2}\mathrm{Re}, \tag{35}$$

$$k_{z_m}\leqslant\frac{3}{8}\frac{\mathrm{Re}^2}{\mathrm{Ha}}. \tag{36}$$

Graphs of relations (32), (35), and (36) are plotted on Figs. 4 and 5, respectively, along with the numerical results of Sec. III C and bring confirmation that the discrete Fourier space can be accurately approached by a continuum.

2. Heuristics on MHD turbulence of Kolmogorov type under strong field

Now, it is worth underlining again that these results are exact, and come exclusively from the mathematical properties of the Navier–Stokes equations, without the involvement of any physical approximation. There is therefore considerable interest in comparing them with orders of magnitude obtained from heuristic considerations. Let us recall how the smallest scales can be obtained in a more physical manner: in a 3D periodic flow where Joule dissipation is stronger than

viscosity except at small scales (Ha≫1), it is usual to consider that a vortex in the inertial range (i.e., not destroyed by viscosity) results from a balance between inertial and Lorentz forces, which implies

$$\frac{k_z}{k_\perp}\sim\left(\frac{\sigma B^2 L}{\rho k_\perp U_v}\right)^{-1/2}. \tag{37}$$

Moreover, one usually assumes that anisotropy remains the same at all scales,[4] over the inertial range. Under this assumption, Eq. (37) implies $U_v(k_\perp)=U_0 k_\perp^{-1}$, where U_0 stands for a typical large scale velocity. This is usually expressed in terms of the energy spectrum as

$$E(k_\perp)\sim k_\perp^{-1}U_v^2(k_\perp)\sim U_0^2 k_\perp^{-3} \tag{38}$$

and allows to rewrite Eq. (37) as

$$\frac{k_z}{k_\perp}\sim\frac{\mathrm{Re}_0^{1/2}}{\mathrm{Ha}}=N^{-1/2}. \tag{39}$$

Re_0 is a Reynolds number scaled on U_0 and L, the ratio $\mathrm{Ha}^2/\mathrm{Re}_0=N$ is the corresponding interaction parameter. Eventually, the small scales are heuristically defined as the smallest possible structures of the inertial range which are not destroyed by viscosity, which means that they result from a balance between inertia and viscosity. This yields

$$\frac{k_{z_m}}{k_{\perp_m}^2}\sim\mathrm{Ha}^{-1}. \tag{40}$$

Now combining Eqs. (39) and (40) yields

$$k_{\perp_{max}}\sim\mathrm{Re}^{1/2}, \tag{41}$$

$$k_{z_{max}}\sim\frac{\mathrm{Re}}{\mathrm{Ha}}, \tag{42}$$

from which the number of degrees of freedom of the flow can be estimated by counting the number of vortices of size $L/k_\perp\times L/k_\perp\times L/k_z$ in a $L\times L\times L$ box:

$$N_f\sim k_\perp^2 k_z\sim\frac{\mathrm{Re}^2}{\mathrm{Ha}}. \tag{43}$$

When comparing N_f to d_M and the heuristic small scales to Eqs. (35) and (36), we see that our mathematical estimates are loose when compared to heuristics because they exhibit a higher exponent of the Reynolds number than the heuristic relations. However, exponents of the Hartmann number match, which suggests that the mathematical study actually captures well the electromagnetic effects in turbulence. This is confirmed by the fact that the sizes of the smallest scales for a given number of modes n are exactly matched by heuristic results presented in this section [Eqs. (33) and (34) can indeed be recovered from Eqs. (40) and (43), considering $n\sim N_f$ vortices in a box]. This, together with the fact that our estimate for the trace of the dissipation corresponds to an achieved extremum suggests that the latter is optimal. Besides, if one considers $d_M\sim N_f\sim\mathrm{Re}^2/\mathrm{Ha}$ as the order of magnitude expected for the attractor dimension, then one should expect the trace of the operator defined by inertial terms to be of the order of $|\mathrm{Tr}(\mathcal{B}(.,\mathbf{u}))|\sim n\,\mathrm{Re}$ for $d_M\sim\mathrm{Re}^2/\mathrm{Ha}$ to be solution of $\mathrm{Tr}((\mathcal{D}_{\mathrm{Ha}}+\mathcal{B}(.,\mathbf{u}))\mathbf{P}_n)=0$. This suggests that the exponent of n is optimal in Eq. (14), whereas the exponent of Re is somewhat too high to match heuristic results valid for MHD turbulence of Kolmogorov type (i.e., with an established turbulent spectrum). Note that $d_M\sim\mathrm{Re}^2/\mathrm{Ha}$ and Eq. (31) yield $\sin\theta_m\sim\sqrt{\mathrm{Re}}/\mathrm{Ha}$ which matches the prediction of Ref. 5 for the Joule cone angle, whereas the rigorous estimate (32) again yields an overestimated exponent for Re but the right one for Ha.

C. 3D turbulence under weak magnetic field (Ha≪1)

1. Analytical estimates

Let us now investigate the case where $-\lambda_m/\mathrm{Ha}^2>1$ (and $\theta_m=\pi/2$) which relates to weakly anisotropic turbulence, as mentioned in Sec. III. After integration in cylindrical coordinates, for $0<\theta<\pi/2$, Eqs. (25) and (26) rewrite, respectively:

$$\frac{n}{\mathrm{Ha}^3}=\frac{\pi}{6}\left(5l\sqrt{l-1}-2\sqrt{l-1}+3l^2\arctan\left(\frac{1}{\sqrt{l-1}}\right)\right), \tag{44}$$

$$\frac{\mathrm{Tr}(\mathcal{D}_{\mathrm{Ha}}\mathbf{P}_n)}{\pi\,\mathrm{Ha}^5}=\frac{14}{15}\sqrt{l-1}-\frac{4}{45}l\sqrt{l-1}-\frac{8}{45}\sqrt{l-1}+\frac{2}{3}l^3\arctan\frac{1}{\sqrt{l-1}}, \tag{45}$$

with $l=-\lambda_m/\mathrm{Ha}^2$. It is here more difficult to the extract analytical expression for $\mathrm{Tr}(\mathcal{D}_{\mathrm{Ha}}\mathbf{P}_n)$ as a function of n and Ha. However, equations can be expanded in powers of l in the limit $l\to\infty$. This corresponds to a flow where inertia is large compared to electromagnetic effects. Keeping only the terms in $l^{3/2}$ and $l^{1/2}$ in the expansion of Eq. (44), l can be expressed as a function of n/Ha^3. Assuming this latter parameter is large as well and keeping the leading two terms yields

$$-\lambda_m\simeq\frac{1}{4}\frac{2}{\pi}n^{2/3}+\frac{1}{3}\mathrm{Ha}^2. \tag{46}$$

Also, keeping the two leading powers of l in the expansion of Eq. (45) and using Eq. (46) yields

$$\mathrm{Tr}(\mathcal{D}_{\mathrm{Ha}}\mathbf{P}_n)\simeq\frac{3}{10}\left(\frac{6}{\pi}\right)^{2/3}n^{5/3}+\frac{2}{3}\mathrm{Ha}^2\,n. \tag{47}$$

As in the case of strong fields, the upper bound for the attractor dimension is obtained by looking for the value of n which annihilates the trace of the evolution operator:

$$d_M\leqslant\frac{15^{3/2}}{162}\sqrt{5}\,\mathrm{Re}^3\left(1-\frac{4}{3}\frac{\mathrm{Ha}^2}{\mathrm{Re}^2}\right)^{3/2}. \tag{48}$$

In a quasi-isotropic flow the set of minimal modes spread in an ellipsoidlike volume of the phase space so that the maximum values of $k_\perp$ and k_z are obtained for $\theta=0$ and $\theta=\pi/2$, respectively:

$$k_{\perp_m}=\sqrt{-\lambda_m}, \tag{49}$$

$$k_{z_m}=\sqrt{-\lambda_m-\mathrm{Ha}^2}. \tag{50}$$

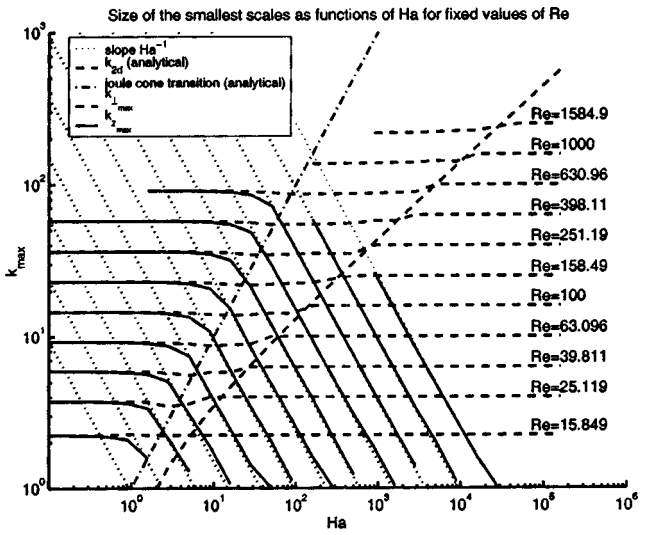

FIG. 5. Size of the smallest scales in the direction of the magnetic field and perpendicular to the magnetic field. Dotted: Ha-1 slope, dashed: k_{2D} analytical, dash-dot: Joule cone transition (analytical), dashed (quasi-horizontal lines): $k_{\perp_{max}}$ (numeric) solid: $k_{z_{max}}$ (numeric).

The bounds for the size of the small scales are obtained by replacing n by d_M in Eq. (46) and using Eqs. (49) and (50), respectively:

$$k_{\perp_m} = \frac{\sqrt{5}}{2\times 3^{5/6}}\mathrm{Re}\left(1-\frac{4}{3}\frac{\mathrm{Ha}^2}{\mathrm{Re}^2}\left(1-\frac{3^{2/3}}{5}\right)\right)^{1/2}, \tag{51}$$

$$k_{z_m} = \frac{\sqrt{5}}{2\times 3^{5/6}}\mathrm{Re}\left(1-\frac{4}{3}\frac{\mathrm{Ha}^2}{\mathrm{Re}^2}\left(1+2\frac{3^{2/3}}{5}\right)\right)^{1/2}. \tag{52}$$

These final results on the dimension of the attractor and associated small scales match well the properties of the flow put in light by the numerical results of Sec. III C: in the limit of low Ha, both d_M, $k_\perp$, and k_{z_m} are weakly dependent on electromagnetic effects. The flow is indeed almost isotropic apart from a slight vortex elongation in the z direction. Also, the upper bound for the attractor dimension in classical 3D turbulence (16) is recovered for Ha$=0$. Note that when Ha is progressively increased from 0, the small scales initially grow both in the direction orthogonal to the field and in the direction of the field. However, the growth is more important in the direction of the field which results in an early anisotropy. It can be seen from Fig. 5 that when Ha is increased up to a value where Lorentz dissipation is more important than viscous dissipation, the length scale in the direction orthogonal to the field saturates at the value found in Eq. (35) whereas the length scale in the direction of the field continues to grow until it reaches the typical macroscopic length scale.

2. Heuristic considerations in quasi-isotropic MHD turbulence of Kolmogorov type

When eletromagnetic effects are small compared to inertia, the turbulence is almost 3D isotropic, so one expects the size of the small scales to be close to the value $k_m^{-1} \sim \mathrm{Re}^{-3/4}$ obtained from the K41 theory.[17] Indeed, Ref. 4 proposes some heuristic estimates which suggest that the size of the small scales if of this order of magnitude, and tends to slightly increase under the effects of small eletromagnetic effects. To this regard, the mathematical estimates (48), (51), and (52) again exhibit higher exponents of Re than heuristic results which suggests inertial effects are overestimated. Indeed, as in the case of strong magnetic fields, our estimate for the trace of the dissipation is optimal, so if one is to trust heuristic values of the small scales, then a better estimate for the trace of the inertial terms is expected to be of the order of $n\,\mathrm{Re}^{3/2}$, which is smaller than Eq. (14). As for strong fields, the exponent of n in Eq. (14) seems to be optimal, whereas the exponent of Re is overestimated. It is however remarkable that the exponent expected from heuristic considerations for a weak field is different than the one which would be expected for strong fields. This suggests finding a better estimate than Eq. (14) for the trace of the inertial terms would require to account for the mode distribution in the Fourier space.

D. The 2D case

For two-dimensional flows (i.e., $\lambda_m \leqslant 2\,\mathrm{Ha}$), the motion equations reduce to the 2D Navier–Stokes equations without magnetic field, as the Lorentz force falls to zero. The dissipation operator is a simpler two-dimensional Laplacian operator, for which the trace of any n dimensional subset of the phase space is bounded by (see, for instance, Ref. 15, or using the approximation of a continuous Fourier space as all along this section)

$$\mathrm{Tr}(\mathcal{D}_{\mathrm{Ha}}\mathbf{P}_n) \leqslant \frac{n^2}{2\pi}, \tag{53}$$

which, together with Eq. (14) leads to an upper bound for the attractor dimension:

$$d_M \leqslant \frac{\pi}{8}\mathrm{Re}^2. \tag{54}$$

The estimate (11) presented in Ref. 15 for d_M is based on an accurate estimate for the 2D inertial terms of the order of $n^{1/2}\mathcal{G}(1+\ln n)^{3/4}$. Although it is difficult to compare the Grashof number $\mathcal{G}=\|\mathbf{f}\|_2/\nu$ (where $\|\mathbf{f}\|_2$ stands for the $\mathcal{L}^2$ norm of the dimensional forcing $\mathbf{f}$) to the Reynolds number, one can be sure that the estimate (54) is rather bad in the 2D case, as it features a much higher exponent of n than the estimate from Ref. 7. This again supports the idea that a sharp estimate for the inertial terms must account for the modes distribution [the estimate by Ref. 7 is derived from the 2D assumption, whereas Eq. (14) is a generic 3D result]. However, as both Eq. (11) and our estimate for the transition between 2D and 3D state (22) are consistent with heuristics one can expect them to yield a realistic transition curve in the ($\mathcal{G}$,Ha) plane. The latter is obtained by noticing that the iso $-\lambda(k_\perp,k_z)$ curves for $k_z=0$ are circles centered on the origin so that under the approximation of a continuous Fourier space, the number of 2D modes is $n_{2D}=2\pi k_{2D}^2$ (the factor 2 is due to the fact that eigenspaces are of dimension 2). Setting n_{2D} to the value of d_{2D} given by Eq. (11) and using Eq. (22) yields the transition curve:

$$(\sqrt{2\,\mathrm{Ha}}-1)^2=\frac{c_1}{2\pi}\mathcal{G}^{2/3}(1+\ln\mathcal{G})^{1/3}. \tag{55}$$

The fact that the transition is expressed using Ha and $\mathcal{G}$ makes it all the more applicable to experimental configurations as it only depends on the control parameters, unlike the Reynolds number which involves a velocity which can be hard to define and sometimes to measure.

V. CONCLUDING REMARKS

We have found a rigorous upper bound for the attractor dimension in low-*Rm* MHD turbulence, which is valid for all values of Ha and Re, and relies solely on the Navier–Stokes equations. This bound is obtained for the set of modes which achieves the minimum of the total dissipation (viscous and Joule). This particular set of modes exhibits most of the well known features of MHD turbulence: quasi-isotropic turbulence close to hydrodynamic turbulence for weak electromagnetic force, strongly anisotropic state (modes inside the Joule cone in the Fourier space) when Joule dissipation is of the order of viscous dissipation, and two-dimensional state when the Joule dissipation is dominant. The related estimates for the small scales and Joule cone angle show the same dependence on Ha as their heuristic counterpart. However, because the estimate we use for the inertial terms is not optimal, the exponent of Re in the final attractor dimension is higher than predicted by heuristic considerations. It is noteworthy that this discrepancy to the heuristics is not the same for the three different kinds of turbulence pointed out above, which are characterized by three very different modes distributions (3D isotropic, 3D anisotropic with Joule cone, and 2D isotropic). This suggests that a better estimate for the inertial terms can be obtained by accounting for the mode distribution in the Fourier space. However, the result found for transition (55) between 2D to 3D turbulence does not suffer form this limitation on the estimation of the inertial terms as it is derived from estimates for inertia and dissipation which both match heuristic results. This simple analytical result now needs testing against experiment.

The other possible improvement to the results found here has to do with the periodical conditions in space. Indeed, in laboratory experiments, as well as industrial setups, the 2D state is achieved when the flow is confined between two walls perpendicular to a strong magnetic field, so that the dissipation along these walls (in the Hartman boundary layer) is often the main factor which determines the whole flow.[18] This makes the 2D state obtained under 3D periodical conditions rather unphysical. A way to improve this result would be to carry out the same study as presented here with walls in $z=0$ and $z=1$. Unfortunately, this will be at the expense of a more complex calculation for which no analytical estimate can be derived.

Eventually, the fact that the least dissipative modes already incorporate many properties of MHD turbulence encourages us to investigate their ability to reproduce the energetic properties of MHD turbulence such as the k^{-3} spectrum observed in the 3D anisotropic regime.[4] Also, it may be possible to reproduce the main properties of the flow using a reduced set of these modes in a numerical model. Indeed, because of the strong anisotropy which characterizes low-*Rm* MHD turbulence under strong magnetic field, it is in principle possible to fully describe this class of flow using $\mathrm{Re}^2/\mathrm{Ha}$ taken from the set of least dissipative modes. This represents a much smaller set of modes than the Re^2 modes obtained by taking all the Fourier modes of wave number smaller than $k_{\perp_m}$.

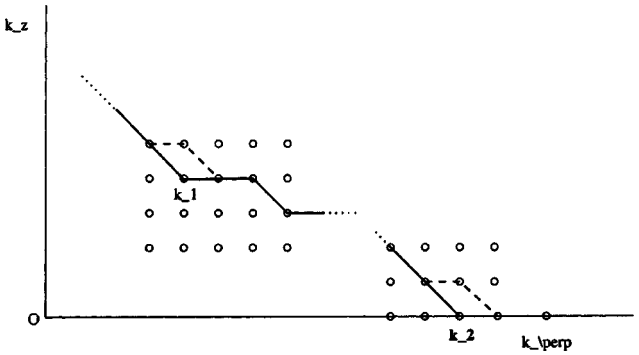

FIG. 6. Recursive process to find the $n+1$st modes knowing the first n ones (located below the solid line, excluding the points on the line). The point $\mathbf{k}_{n+1}$ which yields the minimal dissipation outside of the set made up with the first n modes is found among the points of the solid line. Once it is found by looking at all the values of $-\lambda$ for these points, the $n+2$nd mode is searched among the points of the dashed line, obtained by modifying the solid line so that it "surrounds" $\mathbf{k}_{n+1}$. Two distinct examples are given: $\mathbf{k}_{n+1}=\mathbf{k}_1$ or $\mathbf{k}_{n+1}=\mathbf{k}_2$.

ACKNOWLEDGMENT

The authors would like to acknowledge financial support from the Leverhulme Trust, under Grant No. F/09452/A.

APPENDIX: NUMERICAL CALCULATION OF THE LEAST DISSIPATIVE MODES

The sequence of n eigenmodes of the dissipation operator is calculated recursively, in growing order of the eigenvalues' modulus (which represents the dissipation rate of the associated eigenmodes). We start from the less dissipative mode (1,0) which corresponds to the eigenvalue of smallest module $\lambda_1=-1$ (or smallest dissipation rate). As $(k_\perp,k_z)\mapsto-\lambda(k_\perp,k_z)$ has a unique absolute minimum, at (0,1) the value of $-\lambda(k_\perp,k_z)$ increases along any direction originating from this minimum. The following less dissipative values (along the sequence of modes sorted by growing dissipation rate) are to be sought in the closest possible vicinity of this minimum (bearing in mind that both $k_\perp$ and k_z span a discrete set of positive values). The second $\mathbf{k}$ is then found by looking for the one which yields the smallest value of $-\lambda(k_\perp,k_z)$ among the points "surrounding" the minimum. The process is iterated, replacing the point selected from the previous step in the surrounding curve by the set of points surrounding it (and which are not already in the set of minimal modes) as shown on Fig. 6. Note that this algorithm requires knowledge of the sequence of values of $k_\perp$. The latter is calculated using the same process, applied to the function $(k_x,k_y)\mapsto k_x^2+k_y^2$.

It is straightforward to extract the value of n which corresponds to the first 3D minimal mode: this gives the 2D–3D transition curve in the (n,Ha) plane. In order to save some calculation time, the attractor's dimension is actually worked out at every added mode: indeed, as the estimate is obtained by writing that the expansion of the n-volume in the phase space is the same as the contraction induced by the dissipation, once the maximum trace of the dissipation operator is obtained for a given n, we calculate the value of Re for which n is an upper bound for the attractor dimension by

$$\mathrm{Re}=\sqrt{\frac{-\mathrm{Tr}(D_{\mathrm{Ha}}\mathbf{P}_n)}{n}}. \tag{A1}$$

The process is iterated using a short program written in the MATLAB environment.

[1]P. A. Davidson, *An Introduction to Magnetohydrodynamics* (Cambridge University Press, Cambridge, 2001).
[2]U. Müller and L. Bühler, *Magnetofluid Dynamics in Channels and Containers* (Springer-Verlag, New York, 2001).
[3]H. K. Moffatt, "On the suppression of turbulence by a uniform magnetic field," J. Fluid Mech. **28**, 571 (1967).
[4]A. Alemany, R. Moreau, P. Sulem, and U. Frish, "Influence of an external magnetic field on homogeneous MHD turbulence," J. Mec. **18**, 277 (1979).
[5]J. Sommeria and R. Moreau, "Why, how and when, MHD turbulence becomes two-dimensional," J. Fluid Mech. **118**, 507 (1982).
[6]P. A. Davidson, "The role of angular momentum in the magnetic damping of turbulence," J. Fluid Mech. **336**, 123 (1997).
[7]P. Constantin, C. Foias, and R. Temam, "On the dimension of the attractors in 2D turbulence," Physica D **30**, 284 (1988).
[8]R. H. Kraichnan and D. Montgomery, "Two-dimensional turbulence," Rep. Prog. Phys. **43**, 547 (1980).
[9]P. Constantin, C. Foias, O. P. Mannley, and R. Temam, "Attractors representing turbulent flows," Mem. Am. Math. Soc. **53**, 314 (1985).
[10]P. Constantin, C. Foias, O. P. Mannley, and R. Temam, "Determining modes and fractal dimension of turbulent flows," J. Fluid Mech. **150**, 427 (1985).
[11]M. Sermange and R. Temam, "Some mathematical questions related to the MHD equations," Commun. Pure Appl. Math. **36**, 635 (1983).
[12]J. V. Shebalin, W. H. Matthaeus, and D. Montgomery, "Anisotropy in MHD turbulence due to a mean magnetic field," J. Plasma Phys. **29**, 525 (1983).
[13]P. Constantin, "Collective 1-infinity estimates for families of functions with orthonormal derivatives," Indiana Univ. Math. J. **36**, 603 (1987).
[14]P. H. Roberts, *Introduction to Magnetohydrodynamics* (Longmans, London, 1967).
[15]C. R. Doering and J. D. Gibbons, *Applied Analysis of the Navier–Stokes Equation* (Cambridge University Press, Cambridge, 1995).
[16]P. Constantin and C. Foias, "Global Lyapounov exponents, Kaplan–Yorke formulas and the dimension of the 2D Navier–Stokes equation," Commun. Pure Appl. Math. **38**, 1 (1985).
[17]A. N. Kolmogorov, "Local structure of turbulence in an incompressible fluid at very high Reynolds numbers," Dokl. Akad. Nauk SSSR **30**, 299 (1941).
[18]A. Pothérat, J. Sommeria, and R. Moreau, "An effective two-dimensional model for MHD flows with transverse magnetic field," J. Fluid Mech. **424**, 75 (2000).